The authors congratulate Academician I.L. Eremenko on his 70th birthday

Synthesis and Luminescent Properties of Lanthanide Complexes with Benzothiazolylphenolate and -Naphtholate Ligands

T. V. Balashova[a], *, S. K. Polyakova[a, b], A. A. Kukinov[a, b], I. D. Grishin[b], R. V. Rumyantcev[a], G. K. Fukin[a], V. A. Ilichev[a], and M. N. Bochkarev[a, b]

[a]*Razuvaev Institute of Organometallic Chemistry, Russian Academy of Sciences, Nizhny Novgorod, Russia*
[b]*Lobachevsky State University of Nizhny Novgorod, Nizhny Novgorod, Russia*
*e-mail: petrovsk@iomc.ras.ru

Abstract—Sm, Er, and Yb complexes containing anionic (4,5,6,7-tetrafluorobenzothiazol-2-yl)-2-(3,4,5,6-tetrafluoro)phenolate (SON^F) and 3-(2-benzothiazol-2-yl)-2-naphtholate (NpSON) and neutral 1,10-phenanthroline or 2,2'-bipyridine ligands were synthesized. The structures of complexes $Yb(SON^F)_2$-$(NpSON)(DME)_{1.5}$ (**II**) and previously synthesized $Er(SON^F)_3(DME)$ (**I**) were determined by X-ray diffraction (CIF files CCDC nos. 1972769 and 1972770, respectively). Upon excitation by light at λ 405 nm, all complexes showed luminescence of the ligands and Ln^{3+} ions. The OLED devices based on samarium complexes showed moderate intensi metal-centered emission of moderate intensity at a 19 V voltage.

INTRODUCTION

Among the potential application areas of rare earth metal compounds, development of luminescent materials is a key area, because of the unique ability of Ln^{3+} to generate a narrow-band *f–f* emission. The emission wavelength can vary from near-UV to the near-IR range, depending on the lanthanide nature. Scandium, yttrium, and lanthanum, which have no *f*-electrons, and lutetium with a filled 4*f*-shell do not exhibit metal-centered emission; however, their derivatives are of considerable interest as model compounds and potential fluorophores with ligand-centered emission. Apart from the use of luminescent complexes in biomedicine for diagnosis of diseases and imaging of organs and tissues in living systems [1−4], considerable attention is paid to their use as emission layers in organic light emission diodes (OLEDs) [5−7]. A well known and virtually the only way for increasing the luminescence efficiency of lanthanide ions is to choose ligands able to sensitize the lanthanide luminescence due to the antenna effect. In recent years, attention has been focused on lanthanide complexes emitting in the near-IR range [8], which is related to their use in optical amplifiers [9, 10], laser systems [11], night vision devices, guard devices, and fluorescence immunoassays [12]. The synthesis of IR-emit-ting luminophores is associated with some difficulties, because the energy gap between the ground and excited states of Ln^{3+} in relatively small in this case and, as a consequence, the high-energy vibrations of C−H bonds in the ligands efficiently quench the metal emission. Previously, it was shown that the replacement of CH groups by CF groups can increase the luminescence efficiency by decreasing of the quenching [13, 14].

One more way for increasing the IR efficiency of luminophores is to introduce neutral ligands that would provide high extinction coefficients. One of the most popular neutral ligands for sensitizing luminescence of lanthanide ions is *o*-phenathroline, which has a high molar extinction coefficient [15−18]. In addition, the presence of two nitrogen atoms in the phenathroline molecule ensures the formation of a stable chelate ring with a metal ion and shielding of the metal coordination sphere from water or solvent molecules, which quench the luminescence.

The goal of this work is to synthesize new efficient IR-emitting luminophores, namely, heteroligand Er and Yb complexes and to study their photo- and electroluminescent properties. Samarium complexes were obtained to work out the synthetic procedure.

EXPERIMENTAL

The syntheses were carried out under conditions avoiding contact with oxygen and air moisture using standard Schlenk technique. Dimethoxyethane (DME) and tetrahydrofuran (THF) were dried with sodium benzophenone ketyl by a standard procedure and were condensed in vacuo immediately before the use. The silylamide complexes $Ln[N(SiMe_3)_2]_3$ were prepared by a reported procedure [19], the ligands (2-benzothiazol-2-yl)naphthol (HNpSON) and 2-(3,4,5,6-tetrafluoro-2-hydroxyphenyl)-4,5,6,7-tetrafluorobenzothiazole $[H(SON^F)]$ were synthesized by procedures [20, 21]. 2,2'-Bipyridine (Bipy) and 1,10-phenanthroline (Phen) were commercial chemicals (Aldrich). The complexes $Er(SON^F)_3(DME)$ (**I**) and $Yb(SON^F)_2Cp(DME)$ were synthesized as described previously [22, 23].

Synthesis of $Yb(SON^F)_2(NpSON)(DME)_{1.5}$ (II). A solution of 3-(2-benzothiazol-2-yl)-2-naphthol (65 mg, 0.23 mmol) in DME (5 mL) was added to a solution of $Yb(SON^F)_2Cp(DME)$ (250 mg, 0.23 mmol) in DME (10 mL). The reaction mixture was stirred for 30 min at room temperature. Slow evaporation of volatile products resulted in precipitation of yellow crystals, which were separated by decantation. The solid product was washed with cold DME and dried in vacuo. The yield of **II** was 240 mg (77%).

For $C_{49}H_{25}N_3O_6F_{16}S_3Yb$

Anal. calcd., % C, 44.08 H, 1.71 N, 3.09 S, 7.11 Yb, 12.93

Found, %   C, 44.42 H, 1.90 N, 3.17 S, 7.26 Yb, 13.06

IR (KBr; ν, cm^{-1}): 1652 m, 1627 m, 1589 s, 1347 s, 1315 w, 1260 m, 1186 m, 1142 w, 1128 w, 1088 m, 1051 m, 991 s, 950 m, 888 w, 852 m, 817 w, 752 s, 722 m, 625 w, 466 w.

Synthesis of $Sm(SON^F)_3(Phen)(DME)$ (III). A solution of 2-(3,4,5,6-tetrafluoro-2-hydroxyphenyl)-4,5,6,7-tetrafluorobenzothiazole (114 mg, 0.31 mmol) and Phen (18.5 mg, 0.10 mmol) in DME (10 mL) was added to a solution of $Sm[N(SiMe_3)_2]_3$ (65 mg, 0.10 mmol) in DME (5 mL). The reaction mixture was stirred for 30 min at room temperature and concentrated to 2 mL. The light yellow complex **III** was precipitated by hexane, separated by decantation, washed with cold hexane, and dried in vacuo. The yield of **III** was 112 mg (71%).

For $C_{55}H_{18}N_5O_5F_{24}S_3Sm$

Anal. calcd., % C, 43.20 H, 1.15 N, 4.63 S, 6.32 Sm, 10.39

Found, %   C, 43.14 H, 1.18 N, 4.57 S, 6.28 Sm, 10.43

IR (KBr; ν, cm^{-1}): 1652 m, 1632 av, 1586 av, 1498 s, 1422 m, 1351 w, 1286 w, 1259 m, 1227 w, 1183 w, 1147 w, 1098 w, 1056 w, 1000 s, 881 w, 866 w, 844 m, 817 m, 773 w, 754 m, 656 w, 639 w, 627 w, 525 w,

495 w, 461 w. ^{19}F NMR (376 MHz; THF-d$_8$; 20°C; δ, ppm): −140.8 m, −142.3 m, −149.8 m, −158.2 m, −161.7 m, −162.0 m, −162.2 m, −180.0 m. MALDI MS: (M$^+$) 1071.8 ($Sm(SON^F)_2(Phen)^+$); (M$^-$) 1633.8 $(Sm(SON^F)_4^-)$.

Synthesis of $Sm(SON^F)_3(Bipy)(DME)$ (IV). A solution of 2-(3,4,5,6-tetrafluoro-2-hydroxyphenyl)-4,5,6,7-tetrafluorobenzothiazole (178 mg, 0.50 mmol) and Bipy (25 mg, 0.16 mmol) in DME (10 mL) was added to a solution of $Sm[N(SiMe_3)_2]_3$ (101 mg, 0.16 mmol) in DME (5 mL). The reaction mixture was stirred for 30 min at room temperature and concentrated to 2 mL. The resulting light yellow precipitate of complex **IV** was separated by decantation, washed with cold DME, and dried in vacuo. The yield of **IV** was 170 mg (70%).

For $C_{53}H_{18}N_5O_5F_{24}S_3Sm$

Anal. calcd., % C, 42.18 H, 1.23 N, 4.59 S, 6.41 Sm, 10.68

Found, %   C, 42.23 H, 1.20 N, 4.65 S, 6.38 Sm, 10.61

IR (KBr; ν, cm^{-1}): 1654 m, 1596 m, 1500 s, 1439 s, 1412 w, 1352 m, 1291 w, 1261 m, 1181 m, 1159 w, 1139 w, 1098 m, 1047 w, 998 s, 886 m, 869 w, 820 m, 766 m, 749 m, 654 w, 647 w, 625 w, 615 w, 600 w, 525 w, 498 w, 464 w. ^{19}F NMR (376 MHz; THF-d$_8$, 20°C; δ, ppm): −140.1 m, −140.3 m, −150.5 m, −155.6 m, −161.0 m, −161.6 m, −164.8 m, −178.5 m. MALDI MS: (M$^+$) 1047.7 ($Sm(SON^F)_2(Bipy)^+$); (M$^-$) 1633.8 $(Sm(SON^F)_4^-)$.

Synthesis of $Er(SON^F)_3(Phen)(DME)$ (V) was carried out by a procedure similar to that for the synthesis of **III** using 2-(3,4,5,6-tetrafluoro-2-hydroxyphenyl)-4,5,6,7-tetrafluorobenzothiazole (163 mg, 0.44 mmol), Phen (26 mg, 0.14 mmol), and $Er[N(SiMe_3)_2]_3$ (95 mg, 0.15 mmol) in DME (15 mL). The yield of **V** was 177 mg (78%).

For $C_{55}H_{18}N_5O_5F_{24}S_3Er$

Anal. calcd., % C, 42.64 H, 1.20 N, 4.59 S, 6.57 Er, 10.77

Found, %   C, 42.67 H, 1.17 N, 4.52 S, 6.60 Er, 10.80

The IR spectrum of complex **V** was similar to the spectrum of **III**. MALDI MS: (M$^+$) 1087.9 ($Er(SON^F)_2$-(Phen)$^+$); (M$^-$) 1647.8 $(Er(SON^F))_4^-$.

The IR spectra were measured on an FSM-1201 FT IR spectrometer in the 4000−400 cm^{-1} range (mineral oil mulls). Elemental analysis for C, H, N, S was performed on an Elementar Vario ELcube Analyzer. The absorption spectra were recorded on a Perkin-Elmer 577 spectrometer; the emission spectra in the 200−800 nm range were measured using a Perkin-Elmer LS-55 spectrometer. The electroluminescence spectra and efficiency in the IR range were measured

on a NIR-512 spectrometer (Ocean Optics) calibrated by the LS-1 CAL lamp (Ocean Optics). The ^{19}F NMR spectra were recorded at 376 MHz in THF-d_8 on an Agilent DD2 400 spectrometer.

Mass spectra were recorded using a Bruker Microflex LT mass spectrometer in the linear mode. The sample preparation was as follows: a solid compound (2–5 mg) was spread over a stainless-steel plate by a spatula. A solution (2 µL) of DCTB (trans-2-[3-(4-tert-butylphenyl)-2-methyl-2-propenylidene]malononitrile) (20 mg/mL) in THF was deposited onto the compound covering the plate, then the sample was dried in air for 5–10 s and placed in a spectrometer. The spectra were recorded in the positive or negative ion mode depending on the analyzed compound.

The three-layer OLED devices (organic light emitting diodes) ITO/TPD (25 nm)/complex (45 nm)/BATH (15 nm)/Yb (ITO is indium tin oxide (anode), TPD is N,N'-bis(3-methylphenyl)-N,N'-diphenyl-benzylidene (hole transporting layer), BATH is 4,7-diphenyl-1,10-phenathroline (hole blocking layer), Yb is cathode) were fabricated by successive deposition of nanolayers of organic materials and the ytterbium top contact by thermal evaporation–condensation in vacuo (5×10^{-6} Torr) onto a glass substrate coated by a transparent conducting indium tin oxide ITO (100 nm; surface resistance of 15 Ω/cm^2, Aldrich). The layer thickness was monitored by a calibrated quartz resonator (Quartz crystal monitor Q-pod). The electroluminescence (EL) spectra in the visible region and voltammetric and brightness characteristics were measured for non-encapsulated samples on an USB-2000 fluorometer (Ocean Optics) for the visible range and a NIR-512 instrument (Ocean Optics) for a near-IR range using a PPE 3323 power source (GW Instek) and a GDM 8246 digital multimeter (GW Instek).

X-ray diffraction. The crystallographic data for complexes **I** and **II** were collected on a Bruker D8 Quest diffractometer (graphite monochromator, Mo$K_α$ radiation, λ = 0.71073 Å). The experimental sets of intensities were integrated with a SAINT software program [24]. The SADABS program [25] was used to apply absorption corrections. The structures were solved by the dual-space method using the SHELXT program [26]. Non-hydrogen atoms were refined by full-matrix least-squares method on F_{hkl}^2 in the anisotropic approximation using the SHELXTL program package [27]. The hydrogen atoms were placed into geometrically calculated positions and refined in the riding model. The crystal contains one non-coordinated DME molecule per two molecules of complex **I**. The crystal of complex **I** was refined as a two-component twin with the ~0.92 : 0.08 domain ratio (the twinning matrix was [−1 0 0 0 −1 0 −0.583 −0.699 1]). In the crystal of complex **I**, 2.5 toluene molecules are present per molecule of the complex. The key crystallographic characteristics and structure refinement parameters for **I** and **II** are summarized in Table 1, and the bond lengths and bond angles are given in Table 2.

The structures were deposited with the Cambridge Crystallographic Data Centre (CCDC nos. 1972769 (**II**), 1972770 (**I**); https://www.ccdc.cam.ac.uk/structures/).

RESULTS AND DISCUSSION

The complex Yb(SON^F)$_2$(NpSON)(DME)$_{1.5}$ (**II**) was prepared by the reaction of YbCp(SON^F)$_2$, containing a labile CpYb group, with (2-benzothiazol-2-yl)naphthol in DME (Scheme 1). The reaction easily proceeds at room temperature and gives the product as yellow crystals in 77% yield.
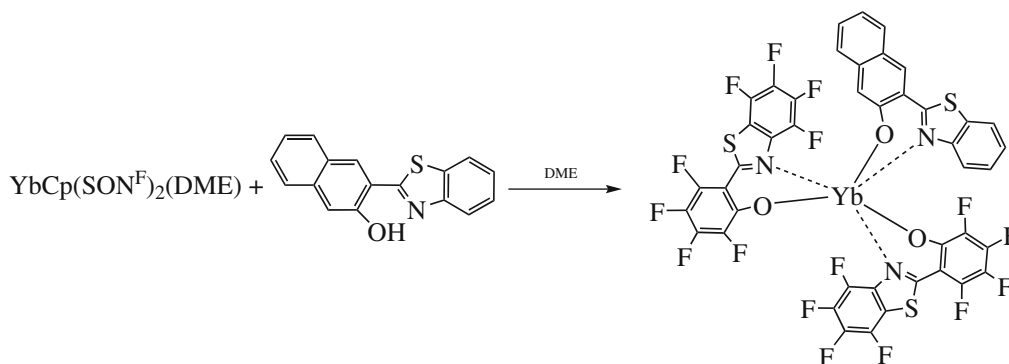
Scheme 1.

According to X-ray diffraction data, the crystal of **II** comprises two independent molecules **A** and **B** with similar molecular structures. The average deviation of non-hydrogen atoms upon superposition of two molecules is 0.270 Å. Since the key geometric characteristics of both molecules are similar (Table 2), below we consider in detail the structure of only molecule **A**. The ytterbium atom in complex **II** is bounded with two

Table 1. Crystallographic characteristics and structure refinement parameters for complexes **I** and **II**

Parameter	Value	
	I	**II**
Molecular formula	$C_{60.50}H_{30}ErF_{24}N_3O_5S_3$	$C_{49}H_{25}F_{16}N_3O_6S_3Yb$
M	1598.31	1324.94
Temperature, K	100(2)	100(2)
System	Triclinic	Triclinic
Space group	$P\bar{1}$	$P\bar{1}$
a, Å	10.6172(7)	13.6813(8)
b, Å	12.9600(8)	13.8163(8)
c, Å	22.9917(14)	25.6341(15)
α, deg	76.210(2)	81.212(2)
β, deg	78.758(2)	78.226(2)
γ, deg	72.119(2)	82.168(3)
V, Å^3	2898.5(3)	4660.1(5)
Z	2	4
ρ(calcd.), mg/m^3	1.831	1.888
μ, mm^{-1}	1.688	2.262
Crystal size, mm	0.25 × 0.21 × 0.12	0.20 × 0.17 × 0.09
$F(000)$	1572	2600
θ, deg	2.243–28.000	2.256–29.999
Number of reflections collected/unique	28946/13641	63520/27132
R_{int}	0.0448	0.0585
R_1, wR_2 ($I > 2\sigma(I)$)	0.0681, 0.01464	0.0467, 0.0756
R_1, wR_2 (for all data)	0.0787, 0.01526	0.0729, 0.0802
S	1.075	1.029
Residual electron density (max/min), e/Å^3	2.064/−2.760	2.062/−1.590

Table 2. Selected bond lengths and bond angles in structures **I** and **II**

| Bond	**I** (Ln = Er)	**II** (Ln = Yb)	
		A	**B**
d, Å			
Ln(1)−O(1)	2.148(5)	2.148(2)	2.161(3)
Ln(1)−O(2)	2.161(5)	2.166(2)	2.152(2)
Ln(1)−O(3)	2.138(5)	2.115(2)	2.119(2)
Ln(1)−O(4)	2.414(5)	2.428(2)	2.387(2)
Ln(1)−O(5)	2.395(5)	2.366(2)	2.402(2)
Ln(1)−N(2)	2.584(6)	2.549(3)	2.577(3)
Ln(1)−N(3)	2.632(6)	2.473(3)	2.492(3)
Ln(1)...S(1)	3.808	3.970	4.046
Angle	ω, deg		
O(2)Yb(1)N(2)	70.55(19)	69.90(9)	69.89(9)
O(3)Yb(1)N(3)	69.2(2)	72.33(9)	72.38(9)
O(1)Yb(1)O(2)	94.4(2)	88.04(9)	84.57(9)
O(1)Yb(1)O(3)	111.3(2)	118.33(9)	119.49(10)
O(2)Yb(1)O(3)	138.22(19)	141.45(9)	144.36(9)
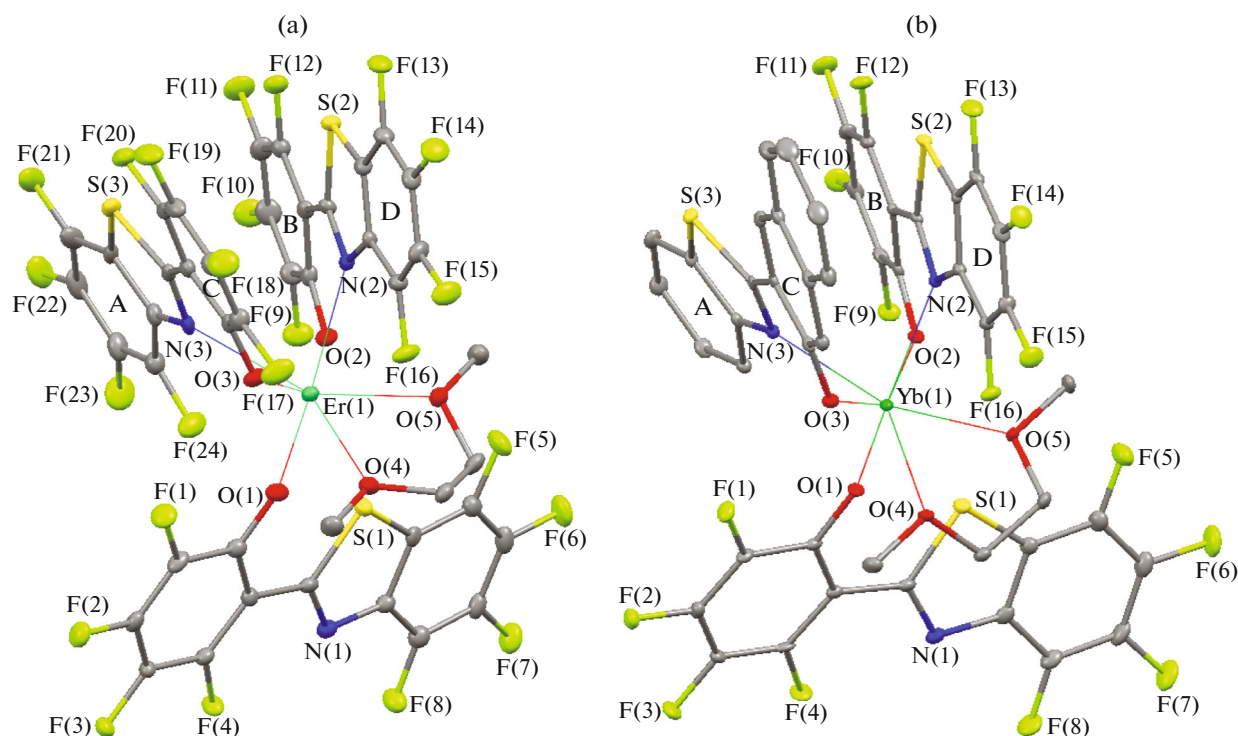
Fig. 1. Molecular structure of complexes (a) **I** and (b) **II**. The thermal ellipsoids are drawn at 30% probability level. The hydrogen atoms are omitted for clarity.

SON^F ligands, NpSON ligand, and neutral DME molecule (Fig. 1b).

The NpSON naphthyl ligand and one of the SON^F ligands have a bidentate coordination via nitrogen and oxygen atoms. The second SON^F ligand is bound to ytterbium in the monodentate fashion via oxygen. The benzothiazolyl moiety of this ligand points to the metal by the sulfur atom; however, the Yb...S distance (3.970 Å) substantially exceeds the sum of the Yb^{3+} ionic radius (R = 0.985 Å) [28] and the van der Waals radius of sulfur (R = 1.8 Å) [29]. Thus, the ytterbium coordination number in complex **II** is seven.

The Yb−O and Yb−N distances in complex **II** vary over narrow ranges (Table 2), typical of related ytterbium complexes [30−32]. Both SON^F ligands and NpSON ligand in complex **II** are non-planar.

The geometric characteristics of the molecules of complex **II** confirms to the existence of π...π interaction between NpSON and bidentately coordinated SON^F. The dihedral angle between the phenolate moiety of SON^F and the benzothiazolyl moiety of NpSON is 20.98°, while the dihedral angle between the NpSON naphtholate moiety and the SON^F benzothiazolyl moiety is 12.14°. The A...B and C...D distances between the centers of the aromatic systems are 3.694 and 3.469 Å, respectively (Fig. 1). In the crystal, molecules **A** and **B** form chains via intermolecular π...π interactions (Fig. 2).

A study of the photoluminescent properties of complex **II** showed that upon laser diode excitation at λ = 405 nm and 300 K, intense luminescence of Yb^{3+} ions (985 nm, $^2F_{5/2} \rightarrow {}^2F_{7/2}$ transition) is observed, apart from the ligand-centered emission (Fig. 3).

It is noteworthy that in the erbium complex Er(SON^F)$_3$(DME) (**I**), prepared previously and isolated from methanol solution, all three SON^F ligands are linked to the metal atom in the bidentate fashion [22]. Meanwhile, as found in the present study, in the crystals of the same complex **I** obtained from a toluene solution, two anionic ligands are coordinated in the bidentate fashion, while the third ligand is bound to Er^{3+} only through the oxygen atom. The sulfur atom of the benzothiazolyl moiety of the monodentately coordinated ligand is directed toward the metal, like in complex **II**. The Er...S distance (3.808 Å) in **I** is somewhat shorter than the Yb...S distance in **II**, but markedly exceeds the sum of the Er^{3+} ionic radius (R = 1.004 Å) [29] and the van der Waals radius of sulfur (R = 1.8 Å) [30]. Thus, the coordination environment of the erbium atom in **I** is similar to that of the Yb atom in **II**.

The Er−O and Er−N distances in complex **I** are comparable or slightly longer than the Yb−O and Yb−N distances in **II** (Table 2), which is consistent with the slight difference between the erbium and ytterbium ionic radii [28]. Like in complex **II**, in complex **I**,
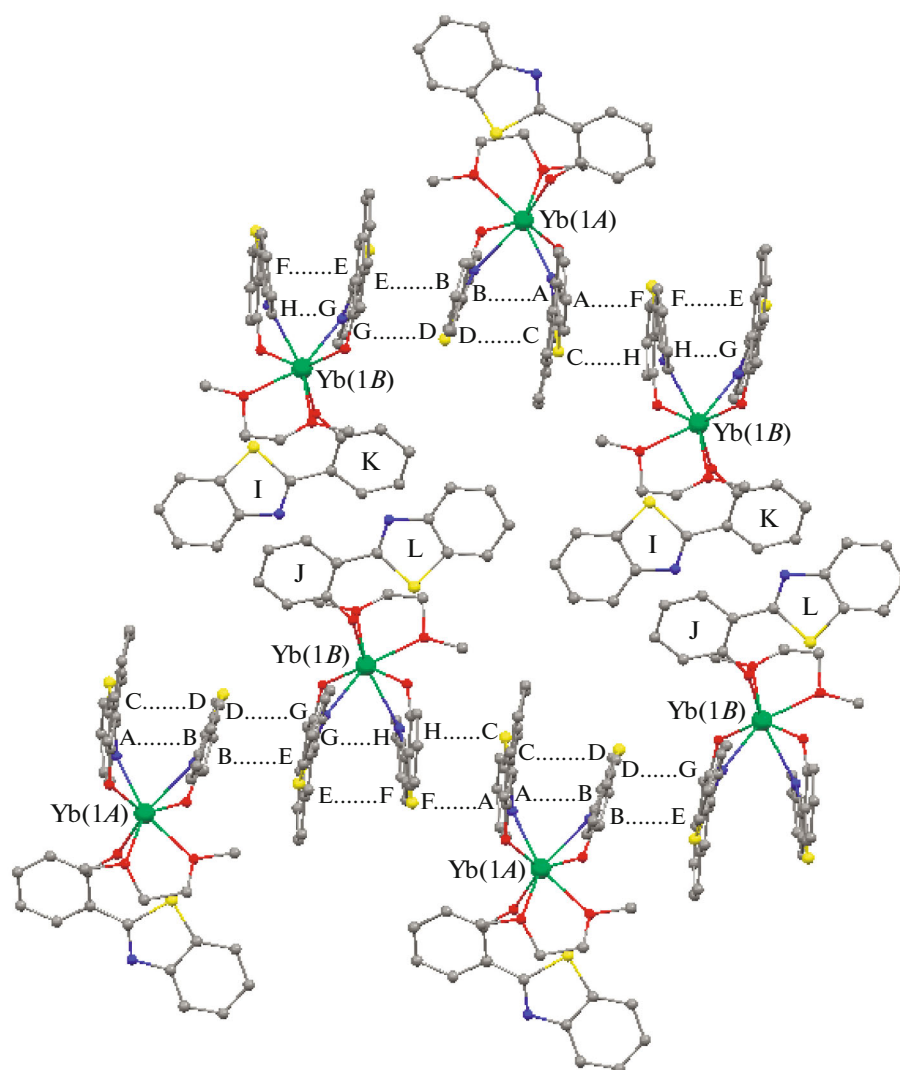
Fig. 2. Fragment of the crystal packing of complex **II**. The designations G, H, E, F of aromatic systems in molecule **B** correspond to designations A, B, C, and D in molecule **A** (Fig. 1). The fluorine and hydrogen atoms are omitted for clarity.
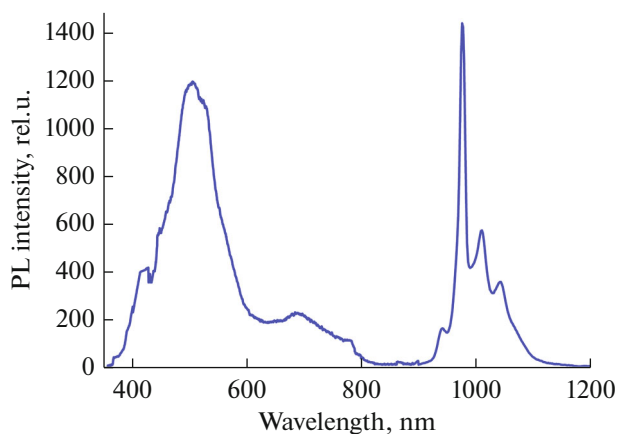

Fig. 3. PL spectra of a solid sample of complex **II** upon laser excitation at $\lambda = 405$ nm (300 K).

intramolecular $\pi...\pi$ interactions are present between the bidentate ligands, as indicated by geometric characteristics of molecules. The dihedral angles between the phenolate and benzothiazolyl moieties of the SON^F ligands are 19.73° and 25.18°. The A...B and C...D distances between the centers of the aromatic systems are 3.597 and 3.678 Å, respectively (Fig. 1a). Furthermore, the arrangement of the molecules of **I** in the crystal confirms to the existence of intermolecular $\pi...\pi$ interactions: the bidentately coordinated SON^F ligands are arranged in such a way that the planes of aromatic rings A and C are virtually parallel to the planes of non-coordinated toluene molecules (the A/E and C/F dihedral angles are 0.32° and 2.98°), while the planes of aromatic rings B and D are slightly rotated relative to the planes of toluene molecules (the B/E and D/F dihedral angles are 21.04° and 21.62°).
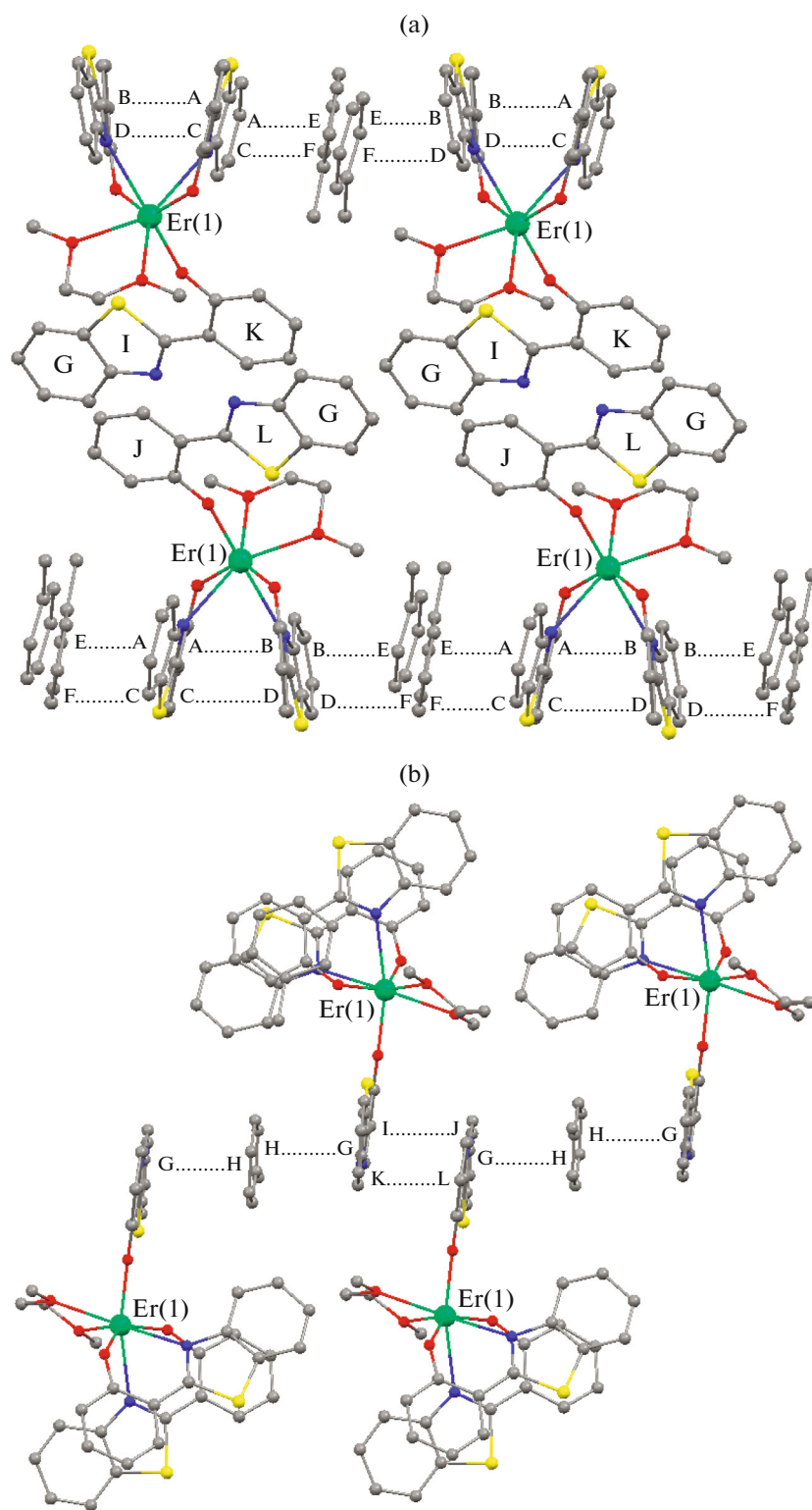
(a)

(b)

Fig. 4. Fragments of the crystal packing of complex **I**. The aromatic systems of toluene molecules in the crystal are noted in the figure by letters E, F, and H. The fluorine and hydrogen atoms are omitted for clarity.
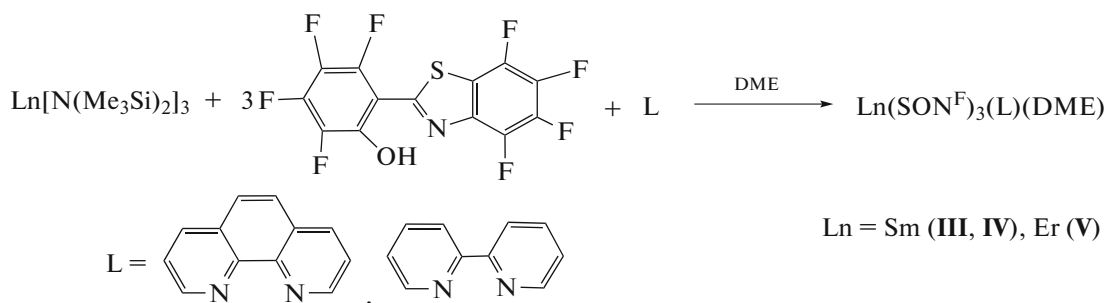
The A...E, C...F, B...E, and D...F distances between the centers of the aromatic moieties are 3.532, 3.416, 3.806, and 3.704 Å, respectively (Fig. 4).

The monodentately coordinated SON^F ligands are virtually parallel to one another and form dimer pairs (Fig. 4a). The intermolecular π...π interactions [33]

connect molecules in the crystal into quasi-infinite chains (Fig. 4b).

It is known that introduction of neutral auxiliary ligands such as Phen and Bipy increases the thermal stability of complexes by saturating the coordination sphere of lanthanide [34] and, as a consequence, preventing the intramolecular F–Ln coordination, which occurs in homoligand complexes [22]. The same technique was used to prepare Sm and Er polyfluorinated benzothiazolate complexes meant for the fabrication of OLED devices by vacuum thermal deposition. Compounds **III**–**V** were prepared by the reaction of $Ln[N(SiMe_3)_2]_3$ with $H(SON^F)$ in DME in the presence of Phen or Bipy (Scheme 2).

$$Ln[N(Me_3Si)_2]_3 \; + \; 3\,H(SON^F) \; + \; L \; \xrightarrow{\;\;DME\;\;} \; Ln(SON^F)_3(L)(DME)$$

$$Ln = Sm \;(\textbf{III, IV}),\; Er \;(\textbf{V})$$

Scheme 2.

Since no crystals of complexes **III**–**V** suitable for X-ray diffraction were obtained, their structure was assumed on the basis of elemental analysis data, IR spectroscopy, and time-of-flight MALDI mass spectrometry. The mass spectrum of complex **V** recorded in the positive-ion mode (Fig. 5a) exhibits signals of the $[(SON^F)_2Er(Phen)]^+$ (1087 Da) resulting from elimination of one ligand. It is noteworthy that the isotopic distribution for the signal is fully consistent with the theoretically calculated one, which can be used to identify the signals.

The negative ion mass spectrum contains signals of the matrix, free charged SON^F ligand, and the signal of the $[(SON^F)_4Er]^-$ anions (1630–1648 Da). The latter are formed upon the replacement of the phenanthroline ligand by the SON^F anion upon laser action on the complex (Fig. 5b). The formation of such anions is characteristic of lanthanide complexes with benzothiazolylphenolate ligands [35, 36] and confirms the proposed structure of **V**.

The negative- and positive-ion mass spectra of samarium compounds **III** and **IV** are similar and contain signals of similar ions with isotopic distributions corresponding to the theoretical one. It is noteworthy that the mass spectra do not exhibit signals for species containing two or more metal ions, which confirms that the complexes are mononuclear.

Thermographic (TG) analysis of erbium complexes showed that the introduction of the Phen molecule, like in other fluorinated lanthanide complexes, significantly increases the thermal stability (Fig. 6).

The absorption spectra of THF solutions of **III** and **IV** at room temperature (Fig. 7) contain bands at 273–290 nm due to π–π^* transitions (B band) and bands at 343–373 nm due to n–π^* transitions. The absorption maxima for complexes **III** and **IV** are shifted with respect to those for the $Sm(SON^F)_3$ complex due to the interligand interaction between SON^F ligands and Phen and Bipy ligands and due to the change in the samarium coordination sphere.

All compounds obtained upon UV excitation exhibit photoluminescence (PL) of ligands as a broad band with a maximum at 480 nm (Fig. 8a). The relative quantum yield is close to 100%. The visible PL spectrum of samarium complex **III** containing a neutral Phen ligand, unlike complex **IV** with Bipy, exhibits bands for metal-centered emission corresponding to $^4G_{5/2} \rightarrow {}^6H_{5/2}$, $^4G_{5/2} \rightarrow {}^6H_{7/2}$, and $^4G_{5/2} \rightarrow {}^6H_{9/2}$ transitions in Sm^{3+} ions, in addition to the ligand bands (Fig. 8a).

The relatively high thermal stability of the complexes with neutral Phen and Bipy ligands allowed using them for the fabrication of OLED devices by vacuum deposition. The electroluminescent properties of the complexes were studied using model three-layer light emitting diodes: ITO/TPD (25 nm)/complex (45 nm)/BATH (15 nm)/Yb. The performance characteristics of the diodes are summarized in Table 3. Contrary to expectations, erbium complex **V** does not show electroluminescence. The EL spectrum of samarium complex **III** contains emission bands characteristic of the Sm^{3+} ion (Fig. 8b).

The current–voltage characteristics (Fig. 9) indicate that complex **III** has lower charge-transport properties than the non-fluorinated analogue [37]. As can be seen from Table 3, OLEDs based on complex **III** show lower brightness and power efficiency, while the current efficiency is somewhat higher than that for OLEDs based on $[Sm(SON)_3]_2$. This behavior can be caused by a change in the energy of the HOMO and LUMO frontier orbitals, resulting in increasing of the optical gap of the complex, which was confirmed by
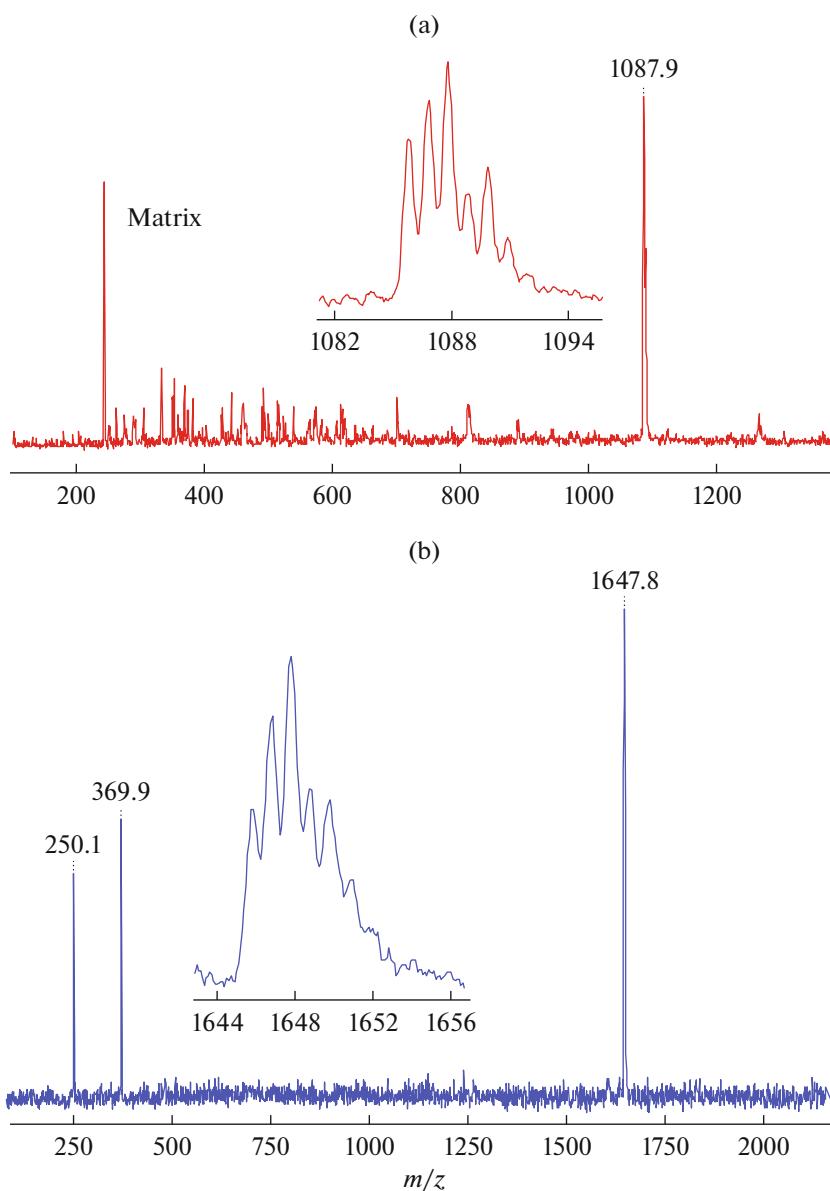
Fig. 5. Mass spectrum of **V** recorded in the (a) positive- and (b) negative-ion modes using DCTB as the matrix.

earlier quantum chemical calculations [22]. It is most likely that higher resistance prevents the increase in brightness and electroluminescence efficiency of lanthanide complexes with perfluorinated ligands, despite the photoluminescent properties of these compounds have better characteristics.

Thus, we synthesized homo- and heteroligand Sm, Er, and Yb complexes containing $H(SON^F)$,

Table 3. Performance characteristics of organic light-emitting diodes

Complex	Turn-on voltage, V*	Maximum brightness (at a voltage), cd/m^2	Current efficiency, cd/A	Power efficiency, lm/W
$[Sm(SON)_3]_2$**	4.8	120(19)	0.12	0.02
$Sm(SON^F)_3(Phen)(DME)$	5.8	17(19)	0.17	0.003

 * For brightness of 1 cd/m^2.
** The characteristics for the complex $[Sm(SON)_3]_2$ were taken from [37].

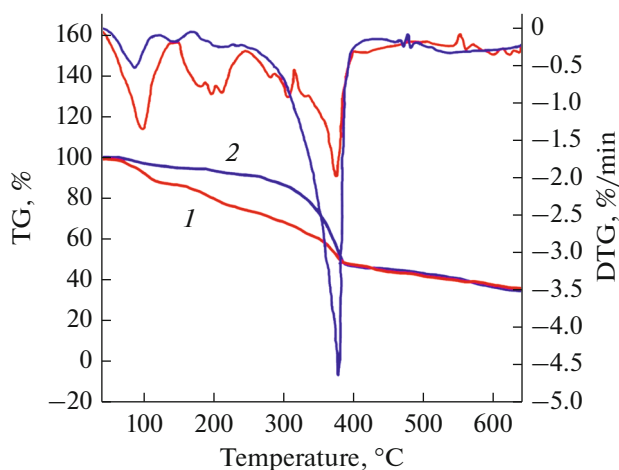**Fig. 6.** TG curves of the complexes (*1*) Er(SON^F)$_3$(DME) and (*2*) Er(SON^F)$_3$(Phen)(DME).

Fig. 7. Absorption spectra of complexes (*1*) Sm-(SON^F)$_3$Bipy, (*2*) (Sm(SON^F)$_3$Phen, (*3*) Sm(SON^F)$_3$ in THF at room temperature (10^{-5} mol/L).

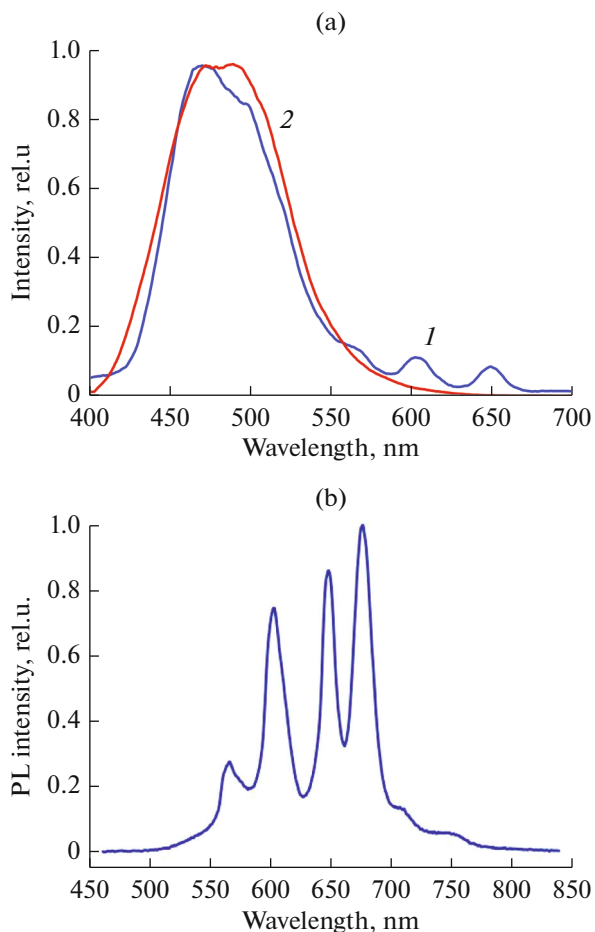H(NpSON), Phen, and Bipy ligands and studied their luminescent properties. The ytterbium complex showed metal-centered emission in the near-IR range caused by *f–f* transitions characteristic of Yb^{3+} ions, which makes it applicable for bioimaging. The Sm complexes possess PL in the visible range. The introduction of N-donor ligands resulted in increasing thermal stability, which made it possible to fabricate a model OLED device based on the samarium complex, demonstrating metal-centered emission of moderate intensity.

Fig. 8. (a) PL spectrum of complexes (*1*) **III** and (*2*) **IV** in THF at λ_{excit} = 380 nm, (b) EL spectrum of complex **III**.
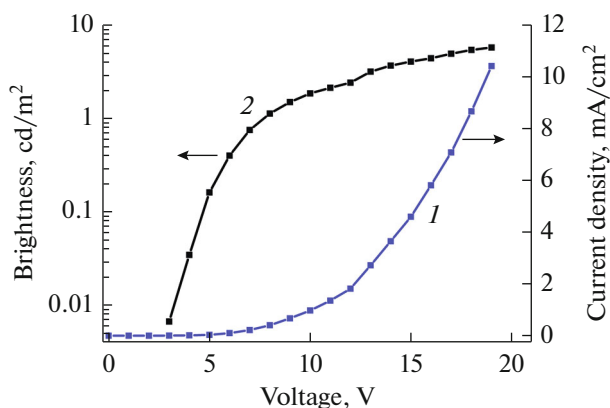
Fig. 9. (*1*) Current−voltage and (*2*) brightness characteristics of complex **III**.

CONFLICT OF INTEREST

The authors declare that they have no conflicts of interest.

REFERENCES

1. New, E.J., Parker, D., Smith, D.G., and Walton, J.W., *Curr. Opin. Chem. Biol.*, 2010, vol. 14, p. 238.
2. Egorova, A.V., Skripinets, Yu.V., Aleksandrova, D.I., and Antonovich, V.P., *Metody i Ob''ekty Khim. Analiza*, 2010, vol. 5, p. 180.
3. Hovinen, J. and Guy, P.M., *Biocojugate Chem.*, 2009, vol. 20, p. 404.
4. Hagan, A.K. and Zuchner, T., *Anal. Bioanal. Chem.*, 2011, vol. 400, p. 2847.
5. Binnemans, K., *Chem. Rev.*, 2009, vol. 109, p. 4283.
6. Eliseeva, S.V. and Bunzli, J.-C., *Chem. Soc. Rev.*, 2010, vol. 39, p. 189.
7. Bochkarev, M.N., Vitukhnovskii, A.G., and Katkova, M.A., *Organicheskie svetoizluchayushchie diody* (OLED) (Organic Light-Emitting Diodes (OLEDs)), Nizhny Novgorod: DEKOM, 2011.
8. Blasse, G. and Grabmaier, B.C., *Luminescent Materials*, Berlin (Germany): Springer, 1994.
9. Sun, R.G., Wang, Y.Z., Zheng, Q.B., et al., *J. Appl. Phys.*, 2000, vol. 87, p. 7589.
10. Kuriki, K., Koike, Y., and Okamoto, Y., *Chem. Rev.*, 2002, vol. 102, p. 2347.
11. Hasegawa, Y., Ohkubo, T., Sogabe, K., et al., *Angew. Chem., Int. Ed. Engl.*, 2000, vol. 39, p. 357.
12. Zhang, J., Badger, P.D., Geib, S.J., and Petoud, S., *Angew. Chem., Int. Ed. Engl.*, 2005, vol. 44, p. 2508.
13. Zheng, Y.X., Lin, J., Liang, Y.J., et al., *J. Mater. Chem.*, 2001, vol. 11, p. 2615.
14. Hasegawa, Y., Kimura, Y., Murakoshi, K., et al., *J. Phys. Chem.*, 1996, vol. 100, p. 10201.
15. Tsaryuk, V., Turowska-Tyrk, I., Legendziewicz, J., et al., *J. Alloys Compd.*, 2002, vol. 341, p. 323.
16. Bünzli, J.-C.G. and Piguet, C., *Chem. Soc. Rev.*, 2005, vol. 34, p. 1048.
17. Zhong, G., Kim, K., and Jin, J.-I., *Synth. Met.*, 2002, vol. 129, p. 193.
18. Armaroli, N., De Cola, L., Balzani, V., et al., *J. Chem. Soc., Faraday Trans.*, 1992, p. 553.
19. Bradley, D.C., Ghotra, J.S., and Hart, F.A., *Dalton Trans.*, 1973, vol. 10, p. 1021.
20. Burin, M.E., Kuzyaev, D.M., Lopatin, M.A., et al., *Synth. Met.*, 2013, vol. 164, p. 55.
21. Li, Z., Dellali, A., Malik, J., et al., *Inorg. Chem.*, 2013, vol. 52, p. 1379.
22. Balashova, T.V., Burin, M.E., Ilichev, V.A., et al., *Molecules*, 2019, vol. 24, p. 2376.
23. Balashova, T.V., Baranov, E.V., Fukin, G.K., et al., *Russ. J. Coord. Chem.*, 2019, vol. 45, p. 712. https://doi.org/10.1134/S107032841909001X
24. *SAINT. Version 8.38A. Data Reduction and Correction Program*, Madison: Bruker AXS Inc., 2012.
25. Krause, L., Herbst-Irmer, R., Sheldrick, G.M., and Stalke, D., *J. Appl. Crystallogr.*, 2015, vol. 48, p. 3.
26. Sheldrick, G.M., *Acta Crystallogr., Sect. A: Found. Adv.*, 2015, vol. 71, p. 3.
27. Sheldrick, G.M., *Acta Crystallogr., Sect. C: Struct. Chem.*, 2015, vol. 71, p. 3.
28. Shannon, R.D., *Acta Crystallogr., Sect. A: Cryst. Phys., Diffr., Theor. Gen. Crystallogr.*, 1976, vol. 32, p. 751.
29. Batsanov, S.S., *Inorg. Mater.*, 2001, vol. 37, p. 871.
30. Aspinall, H.C., Bacsa, J., Beckingham, O.D., et al., *Dalton Trans.*, 2014, vol. 43, p. 1434.
31. Balashova, T.V., Pushkarev, A.P., Rumyantcev, R.V., et al., *J. Organomet. Chem.*, 2015, vol. 777, p. 42.
32. Balashova, T.V., Ilichev, V.A., Grishin, I.D., et al., *Inorg. Chim. Acta*, 2018, vol. 483, p. 379.
33. Janiak, C., *Dalton Trans.*, 2000, no. 21, p. 3885.
34. Pushkarev, A.P., Ilichev, V.A., Maleev, A.A., et al., *J. Mater. Chem. C*, 2014, vol. 2, no. 8, p. 1532.
35. Balashova, T.V., Ilichev, V.A., Grishin, I.D., et al., *Inorg. Chim. Acta*, 2018, vol. 483, p. 379.
36. Balashova, T.V., Pushkarev, A.P., Il'ichev, V.A., et al., *Russ. Chem. Bull.*, 2016, vol. 65, no. 7, p. 1739.
37. Balashova, T.V., Pushkarev, A.P., Il'ichev, V.A., et al., *Polyhedron*, 2013, vol. 50, p. 112.

Translated by Z. Svitanko